SRTTU
Journal of Computational and Applied Research in Mechanical Engineering
jcarme.sru.ac.ir
JCARME
ISSN: 2228-7922

Research Paper

Novel numerical solution of non-linear heat transfer of nanofluid over a porous cylinder: Buongiorno-Forchheimer model

B. Vasu*, [a] and Atul Kumar Ray[b]

[a]*Department of Mathematics, Motilal Nehru National Institute of Technology Allahabad, Prayagraj-211004, India*
[b]*Department of Basic Sciences, Government College of Engineering Keonjhar, Keonjhar-758002, Odisha, India*

Article info:

Article history:

Received: 31/10/2018
Revised: 26/05/2019
Accepted: 30/05/2019
Online: 02/06/2019

Keywords:

Heat transfer,
Porous medium,
Buongiorno model,
Forchheimer number,
Keller-box implicit code.

***Corresponding author:**
bvasu@mnnit.ac.in

Abstract

This study aims to numerically investigate a two dimensional and steady heat transfer over a cylinder in a porous medium with suspending nanoparticles. Buongiorno model is adopted for nanofluid transport on a free convection flow taking the slip mechanism of Brownian motion and thermophoresis into account. The Boussinesq approximation is considered to account for buoyancy. The boundary layer conservation equations are transformed into dimensionless and then elucidated using a robust Keller-box implicit code numerically. The numerical results are displayed graphically and deliberated quantitatively for various values of thermo-physical parameters. Our results shows that, increasing the Forchheimer parameter, Λ, clearly swamps the nanofluid momentum development, decreases the flow for some distance near the cylinder viscous region, later it reverses the trend, and asymptotically reaches the far field flow velocity. Furthermore, as thermophoresis parameter increases, the heat transfer and nanoparticle volume concentration increase within the boundary layer. The present results are validated with the available results of a similar study and is found to be in good coincidence. The study finds applications in heat exchangers technology, materials processing, and geothermal energy storage etc.

1. Introduction

Enhancement of heat transfer in engineering applicants is very important because conventional fluid such as oil, water that are used in engineering applications possess less thermal conductivity. Thermal enhancement of convectional fluids can be upgraded by dispersion of nano-sized particles into the convectional fluids. The resultant combination of convectional fluid (base fluid) and nano-sized particles (nanoparticles) is known as nanofluid [1]. Recently, the studies of nanofluid flows have reported significantly in thermal sciences due to their thermal performance relative to the regular fluids as Wang and Wu reported [2-3]. Numerous models such as the single-phase model [1], the dispersion model [4], and the non-homogeneous two-component model [5] have been developed to study the transport of nanofluid. Specifically, the Buongiorno nanofluid transport model is developed on the basis of the slip mechanism of the nanoparticle with respect to the relative velocity. By means of this model, Beg et al. [6] presented a mathematical model for a nanofluid transport past a vertical wall with oxytactic microorganisms. Das et al. [7] investigated the heat source/sink on a transient laminar magnetic field with nanoparticle flow using a conventional single-phase (homogeneous) model. Sheikholeslami and Ganji [8], presented a review on the transport of nanofluid and heat transfer. Gorla et al. [9] studied the MHD flow of dusty fluid with nanoparticles saturated in a porous medium. Murthy et al. [10] considered the transport of nanofluid embedding non-Darcy porous medium. Besthapu et al. [11] studied the mixed convection flow with nanoparticles taking thermal stratification and viscous dissipation into account numerically. Aly [12] examined the free convection of nanofluid flow over a circular cylinder where the walls are passively controlled in a porous enclosure using a finite volume method. Most recently, Ahmadi et al. [13] studied the thermal conductivity of CuO/EG nanofluid by employing a group method of data handling and genetic algorithm approaches. More works of nanofluids flow and heat transfer analysis can be found in the literature [14, 15].

Transport phenomena in porous media constitute numerous important flow regimes in many branches of engineering and applied physics. The vast majority of models have considered isotropic and homogenous porous media, usually employing the Darcy law, which is effective for low velocity and viscous-dominated flows. It is known that the porous media are heterogeneous and yield variable porosity. Initially, Roblee et al. [16] studied the flow through media of variable radial porosity in the chemical engineering system. Later Vafai [17] studied a theoretical study in a porous region with inertial forces (Forchheimer drag), also presented experimental results in detail. Zueco et al. [18] employed a network simulation method to study the MHD effect on a porous microstructural liquid stream with Darcy-Forchheimer forces. An interesting investigation on the natural convection in Darcian porous media was given by Minkowycz and Cheng [19]. Hamzeh et al. [20] studied the heat transfer and fluid flow past of a sphere. Kumari and Gorla [21] investigated the Magneto-convection flow with suspending nanoparticles past a wedge in non-Newtonian fluid. Kameswaran et al. [22] showed a mixed convection flow of nanofluid over porous wavy surface. Beg et al. [23] studied numerically the flow in orthotropic Darcian porous media from a rotating cone. Very recently, Vasu et al. [24] investigated the entropy generation analysis in a porous medium taking thermally stratification into account. Bég et al. [25] investigated heat transfer and fluid flow over an inclined plate numerically taking Soret/Dufour effects into account. Munawar et al. [26] and Yih [27] discussed the laminar heat transfer flow over a cylinder embedding porous regime. Prasad et al. [28] presented a numerical study for the multiphysical flow of fluid over a cylinder saturating in a variable porosity. Vasu et al. [29] analyzed the influence of Soret and Dufour on magnetic heat transfer flow over a sphere in a porous medium. Satya Narayana and Venkateswarlu [30] presented a numerical solution for a transient MHD natural convection of a nanofluid past a porous plate in a rotating system. Satya Narayana et al. [31] presented an MHD heat transfer with thermal radiation of nanofluid in a porous rotating domain numerically. Harish Babu et al. [32] considered a steady magnetic flow of a Jeffery nanofluid using a non-homogeneous model.

Motivating the above studies and vital application of nanofluid flow in the porous regime, the main purpose of the current study is to analyze the steady viscous incompressible flow of a nanofluid in a non-Darcy porous medium over a horizontal cylinder numerically. The finite-difference results through the Keller-box scheme are presented for highly influential thermophysical parameters. The study has wide applications in heat exchangers, materials processing, and geothermal energy storage, etc.

2. Mathematical formulation

Consider a 2-D incompressible free convection laminar flow of nanofluid over a non-Darcy porous horizontal cylinder. Fig. 1 shows the graphical flow configuration. a denotes the radius of the cylinder. The coordinates x and y are determined along the perimeter of a circular cylinder and normal to the surface, respectively. $\Phi = x/a$ is an angle between the y-axis and the vertically downward line from the center of cylinder $(0 \le \Phi \le \pi)$ shown in Fig. 1. $\boldsymbol{g}$, acts downwards. $T_w(>T_\infty)$ and $C_w(>C_\infty)$ are wall temperature and concentration of the horizontal cylinder, respectively. They are more than the far-field temperature and concentration.

Governing conservation equations as below [5, 14, 15, 27]:

Continuity equation:

$$\nabla.\mathbf{v}=0 \tag{1}$$

Momentum equation:

$$\frac{\rho_f}{\varepsilon}\frac{\partial \mathbf{v}}{\partial t}=-\nabla p-\frac{\mu}{K}\mathbf{v}-\Gamma \mathbf{v}^2$$
$$+\left[C\rho_p+(1-C)\left\{\rho_f\left(1-\beta\left(T-T_\infty\right)\right)\right\}\sin\left(x/a\right)\right]g \tag{2}$$

Energy equation:

$$(\rho c)_m\frac{\partial T}{\partial t}+(\rho c)_f\,\mathbf{v}.\nabla T=k_m\nabla^2 T$$
$$+\varepsilon(\rho c)_p\left[D_B\nabla C.\nabla T+\left(D_T/T_\infty\right)\nabla T.\nabla T\right] \tag{3}$$

Concentration equation:

$$\frac{\partial C}{\partial t}+\frac{1}{\varepsilon}\mathbf{v}.\nabla C=D_B\nabla^2 C+\left(D_T/T_\infty\right)\nabla^2 T \tag{4}$$

Boundary conditions:

$$\text{At } y=0,\ \ u=0,\ v=0,\ \ T=T_w,\ C=C_w \tag{5}$$
$$\text{As } y\to\infty,\ \ \ u=0,\ T\to T_\infty,\ C\to C_\infty \tag{6}$$

It can be writeen $\mathbf{v}=(u,v)$.

In the above equations, μ is the dynamic viscosity, ρ_f and ρ_p are the fluid density and density of particle, respectively, β is the fluid's volume expansion coefficient, $(\rho c)_m$ is the heat capacity, D_B and D_T are the coefficient of Brownian diffusion and coefficient of thermophoretic diffusion, respectively, k_m is the thermal conductivity, and g is the gravity.

The momentum equation (Eq. (2)) can be written by using the proper value of reference pressure, as:

$$\nabla p+\frac{\mu}{K}\mathbf{v}+\Gamma\mathbf{v}^2=\left[\left(1-C_\infty\right)\rho_{f\infty}\beta\left(T-T_\infty\right)\sin\left(x/a\right)\right.$$
$$\left.+\left(\rho_p-\rho_{f\infty}\right)\left(C-C_\infty\right)\sin\left(x/a\right)\right]g \tag{7}$$

By means of the boundary-layer approximation and Boussinesq approximation, Eqs. (1-4) which govern the flow are reduced to:

$$\frac{\partial u}{\partial x}+\frac{\partial v}{\partial y}=0 \tag{8}$$

$$u\frac{\partial u}{\partial x}+v\frac{\partial u}{\partial y}=\left[\left(1-C_\infty\right)\rho_{f\infty}\beta g\left(T-T_\infty\right)\sin\left(x/a\right)\right.$$
$$\left.-\left(\rho_p-\rho_{f\infty}\right)g\left(C-C_\infty\right)\sin\left(x/a\right)\right]+\nu\frac{\partial^2 u}{\partial y^2}-\frac{\nu}{K}u-\Gamma u^2 \tag{9}$$

$$u\frac{\partial T}{\partial x}+v\frac{\partial T}{\partial y}=\alpha_m\nabla^2 T$$
$$+\tau\left[D_B\frac{\partial C}{\partial y}\frac{\partial T}{\partial y}+\left(\frac{D_T}{T_\infty}\right)\left(\frac{\partial T}{\partial y}\right)^2\right] \tag{10}$$

$$\frac{1}{\varepsilon}\left(u\frac{\partial C}{\partial x}+v\frac{\partial C}{\partial y}\right)=D_B\frac{\partial^2 C}{\partial y^2}+\left(\frac{D_T}{T_\infty}\right)\frac{\partial^2 T}{\partial y^2} \tag{11}$$

where

$$\alpha_m=\frac{k_m}{(\rho c)_f},\qquad \tau=\frac{(\rho c)_p}{(\rho c)_f}$$

Introducing a stream function ψ defined by:

$$u=\frac{\partial\psi}{\partial y},\quad v=-\frac{\partial\psi}{\partial x}.$$

So, Eq. (8) is satisfied identically.

Introducing the suitable dimensionless variables:

$$\xi=\frac{x}{a},\ \eta=\frac{y}{a}\sqrt[4]{Gr},\ f(\xi,\eta)=\frac{\psi}{\nu\xi\sqrt[4]{Gr}}$$

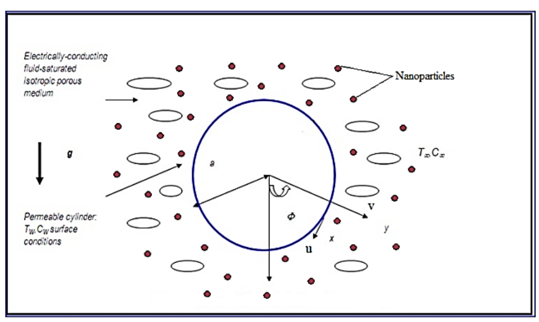

Fig. 1. Schematic of flow configuration.

$$\theta(\xi,\eta)=\frac{T-T_\infty}{T_w-T_\infty},\phi(\xi,\eta)=\frac{C-C_\infty}{C_w-C_\infty},\quad (12)$$
$$Gr=\frac{(1-\phi_\infty)\rho_{f\infty}g\beta(T_w-T_\infty)a^3}{\nu^2}$$

Using dimensionless variables, Eqs. (8-11), are obtained in the dimensionless forms as follows:

$$f'''+ff''-(1+\xi\Lambda)f'^2+\frac{\sin\xi}{\xi}(\theta-Nr\phi) -\frac{1}{DaGr^{1/2}}f'=\xi(f'\frac{\partial f'}{\partial\xi}-f''\frac{\partial f}{\partial\xi}) \quad (13)$$

$$\frac{\theta''}{\Pr}+f\theta'+Nb\theta'\phi'+Nt(\theta')^2=\xi(f'\frac{\partial\theta}{\partial\xi}-\theta'\frac{\partial f}{\partial\xi}) \quad (14)$$

$$\phi''+Scf\phi'+\left(\frac{Nt}{Nb}\right)\theta''=\xi(f'\frac{\partial\phi}{\partial\xi}-\phi'\frac{\partial f}{\partial\xi}) \quad (15)$$

The transformed dimensionless boundary conditions are:

$$\eta=0:\quad f'=0,\quad f=0,\quad \theta=1,\quad \phi=1 \quad (16a)$$
$$\eta\to\infty:\quad f'\to0,\quad \theta\to0,\quad \phi\to0 \quad (16b)$$

where Φ is the azimuthal coordinate, ξ is the non-dimensional tangential coordinate, $\Lambda=\Gamma a$ is the non-Darcy parameter, $Da=\frac{K}{a^2}$ is a Darcy parameter, $\Pr=\frac{\nu}{\alpha_m}$ is the Prandtl number, $Nr=\frac{(\rho_p-\rho_{f\infty})(C_w-C_\infty)}{\rho_{f\infty}(1-C_\infty)\beta(T-T_\infty)}$ is the buoyancy ratio parameter, $Sc=\frac{\nu}{D_m\varepsilon}$, $Nb=\frac{\tau D_B(C_w-C_\infty)}{\nu}$ and $Nt=\frac{\tau D_T(T_w-T_\infty)}{\nu T_\infty}$ are respectively the Schmidt number, Brownian motion and thermophoresis parameters.

For the quantities of physical choice, the coefficient of skin-friction, local Nusselt, and Sherwood number are calculated as:

$$\frac{1}{2}C_f\sqrt[4]{Gr}=\xi f''(\xi,0) \quad (17a)$$

$$\frac{Nu}{\sqrt[4]{Gr}}=-\theta'(\xi,0) \quad (17b)$$

$$\frac{Sh}{\sqrt[4]{Gr}}=-\phi'(\xi,0) \quad (17c)$$

3. Solution using Keller-box finite-difference code

The numerical analysis integrates the non-dimensional Eqs. (13-15) subjected to the boundary conditions (16) by an implicit finite-difference approximation with an efficient finite-difference scheme Keller-box method [33], described by Cebeci and Bradshaw [34]. The scheme is unconditionally stable. This method has been employed for various complex domains like aerodynamic problems [35, 36], heat transfer in a porous regime [37, 38], and heat and mass transfer in a micropolar regime [39-41] have employed to study an unsteady heat transfer of a non-Newtonian nanofluid. The numerical method is not described for the sake of concision. The solution process of the Keller-box method is given in many references including Gorla and Vasu [40]. Because of the conservation of space, the detailed solution is omitted here. Considered a uniform grid of size 1501 ×31 in the η-ξ region. Computations are carried out with $\Delta\xi=0.1$, and $\Delta\eta=0.002$. For the desired accuracy, convergence criterion is fixed at 10^{-5} as the change between any two successive iterations. Fig. 2 shows the representation of the computational cells for the Keller-box method after meshing. The results are also shown to be grid-independent.

4. Numerical validations

In order to judge the validation of numerical outcomes, the current results of the local heat transfer coefficient ($-\theta'(\xi,0)$) are compared with results of Merkin [42] and Yih [27] for various values of ξ, for $Da\to\infty$, $\Lambda=0$, $\Pr=Gr=1, Nt=Nb=Nr=0, f_w=0, Sc=0.$ Table 1 shows the validation of present result by assuming that the porous field and nanofluid effects are negated in the models. It is found that the current numerical solution is in good compliance. Further, the local heat transfer coefficient ($-\theta'(\xi,0)$) is decreased along the edge of the cylinder. Hence a very strong thermal enhancement (θ) is achieved past a circular cylinder.

5. Results and discussion

This section focuses on the physical insight through numerical results of nanofluid transport over a cylinder in a non-Darcy porous regime taking the Buongiorno-Forchheimer model into account. The numerically computed results for velocity, temperature, coefficient of skin-friction, local Nusselt number, nanoparticle volume concentration, and local Sherwood number for different values of dimensionless thermophysical parameters viz., Nb, Nt, Nr, Λ, Da, Sc, $\Pr$, tangential coordinate (ξ) are presented along the radial coordinate (η) in form of tables and figures. The numerical results are validated and verified through a comparison made with previously reported work. The comparisons are found to be in excellent compliance (See Section 4).

The effect of varying Λ and Pr on the coefficient of skin friction, heat transfer, and nanoparticle volume fraction coefficient are presented in Table 2. It is found that skin friction and coefficients of nanoparticle volume fraction increase, whereas heat transfer coefficients reduce along the tangential coordinate (ξ) for Λ and Pr. It is worth mention that thermal enhancement occurs due to the presence of nanoparticles. With increasing Pr, the values of $-\theta'(\xi,0)$ significantly increase, whereas $f''(\xi,0)$ and $-\phi'(\xi,0)$ values decrease. The same tendency is observed and in good coincidence with the earlier results by Prasad *et al.* [38]. Also it is found that the reduction of skin friction values and heat transfer coefficients are happens due to increasing Forchheimer parameter. The reverse trend is observed for the local mass transfer coefficients.

Figs. 3-5 describes the influence of Nb on velocity (f'), temperature (θ), and nanoparticle volume concentration (ϕ) for water-based nanofluids over the horizontal circular cylinder regime. Enlarging Nb leads to a rise in velocity as well as temperature whereas the opposite trend is observed for nanoparticle volume fraction concentration (ϕ).

Larger values of the Nb approach to smaller nano-particles [5] and this boosts acceleration of the hydrodynamics. Also $\phi(\eta)$ decreases with increase in the Nb. Figs. 6-8 shows the numerical result of the thermophoresis on velocity (f'), temperature (θ), and nanoparticle volume concentration (ϕ). Moving of the particles in the way of shrinking temperature due to thermal gradient forces, the phenomenon is called thermophoresis.

The thermophoretic parameter (Nt) involves in Eqs. (14 and 15), and it plays a significantly influential in the thermal diffusion and nanoparticle diffusion in the domain. As Nt increases, the velocity of nanofluid decreases. It is also witnessed from Figs. 7 and 8 that, a rise in Nt leads to thermal enhancement and nanoparticle concentration increase, *i.e.*, thermal and nanofluid volume fraction boundary layer increase, so that the thermal layer raises.

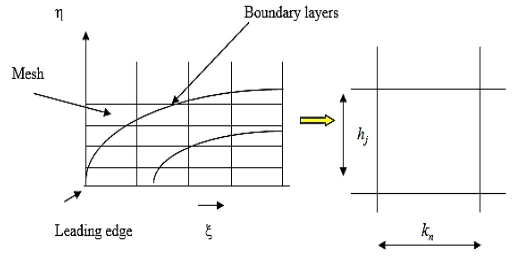

Fig. 2. Meshing and computational cell.

Table 1. Comparison of ($-\theta'(\xi,0)$) for various values of ξ for $Da \to \infty$, $\Lambda = 0$, $\Pr = Gr = 1$, $Nt = Nb = Nr = 0$, $f_w = 0$, *and* $Sc = 0$.

ξ	$-\theta'(\xi,0)$		
	Merkin [42]	**Yih [27]**	**Present results**
0.0	0.4212	0.4214	0.42145
0.4	0.4182	0.4184	0.41835
0.8	0.4093	0.4096	0.40897
1.2	0.3942	0.3950	0.39532
1.6	0.3727	0.3740	0.37451
2.0	0.3443	0.3457	0.34660
2.4	0.3073	0.3086	0.30897
2.8	0.2581	0.2595	0.25917
π	0.1963	0.1962	0.19654

Larger thermophoresis indicates the durable movement of nano-particles with respect to the rate of heat temperature away from the cylinder surface.

Figs. 9-11 demonstrate the impact of the buoyancy ratio parameter on velocity (f'), temperature (θ), and nanoparticle volume concentration (ϕ) for water-based nanofluid. With increasing Nr values, the velocity profile is strongly decreases in the boundary layer; the tendency of velocity in Fig. 9 can be seen. However, from Figs. 10 and 11, the opposite behavior is seen in profiles of temperature θ and nanoparticle concentration ϕ.

Figs. 12-14 display the influence of Forchheimer inertial parameter (Λ) on the flow variables, velocity (f'), temperature (θ), and nanoparticle volume concentration (ϕ) in the boundary layer regime of nanofluid flow past a cylinder. Quadratic Forchheimer drag appears in Eq. (13) and is directly proportional to Λ.

Form Fig. 12, it is evident that increasing Λ clearly floods the nanofluid momentum development, and decreases the flow for some distance near the cylinder viscous region, later it reverses the trend and asymptotically reaches the far-field flow velocity. Also, it is found that an increase in Λ enhances thermal boundary layer thickness and nanoparticle concentration.

Figs. 15-17 depict the hydrodynamics, heat transfer, and nanofluid volume fraction behavior past the cylinder for different values of ξ. Velocity clearly slows down with increasing ξ values (Fig. 15) for some distance. Conversely, a large increase in θ and ϕ occurs with increasing ξ values, as shown in Figs. 16 and 17.

Temperature and nanofluid volume fraction are both enhanced.

The influence of Nb and Nt on $f''(\xi,0)$, $-\theta'(\xi,0)$ and $-\phi'(\xi,0)$ over cylinder surface are presented in Figs. 18–20 and Figs. 21–23, respectively. With increasing influential nanofluid slip parameters (Nb and Nt), corresponding $f''(\xi,0)$, $-\theta'(\xi,0)$ and $-\phi'(\xi,0)$ are consistently enhanced. It implies that the gradients of flow are considerably increased along the surface of cylinder.

It is worth to mention that the enhancement occurs due to the presence of nanoparticles in the boundary layer regime. Figs. 24–26 depicts the distribution of $f''(\xi,0)$, $-\theta'(\xi,0)$ and $-\phi'(\xi,0)$ along the cylinder periphery (ξ coordinate) for various values buoyancy ration parameter (Nr). For increasing Nr, corresponding to lesser influences of flow gradient, wall shear stress is steadily condensed. With growing Nr, the local Nusselt number, and local Sherwood number considerably decreases and increases, respectively. For increasing Nr, corresponding to lesser influences of flow gradient, wall shear stress is steadily condensed. With growing Nr, the local Nusselt number, and local Sherwood number considerably decreases and increases, respectively.

Table 2. Values of skin friction coefficient $f''(\xi,0)$, heat transfer coefficient $-\theta'(\xi,0)$ and nanoparticle volume fraction coefficient $-\phi'(\xi,0)$ for different values of Prandtl number Pr, non-Darcy parameter Λ and tangential coordinate ξ when Gr = 1, Nt = Nr = Nb = 10^{-5}, Da = 0.1, Sc = 0.6.

		$\xi=0.0$			$\xi=0.5$			$\xi=1.0$		
Λ	Pr	$f''(\xi,0)$	$-\theta'(\xi,0)$	$-\phi'(\xi,0)$	$f''(\xi,0)$	$-\theta'(\xi,0)$	$-\phi'(\xi,0)$	$f''(\xi,0)$	$-\theta'(\xi,0)$	$-\phi'(\xi,0)$
0.1	1	0	0.1894	0.0635	0.1414	0.1837	0.0639	0.2471	0.1688	0.0651
	10	0	0.4980	-0.2714	0.1278	0.4845	-0.2600	0.2250	0.4486	-0.2300
	100	0	1.1911	-0.9808	0.1021	1.1652	-0.9561	0.1815	1.0956	-0.8876
	1000	0	2.5048	-2.3011	0.0712	2.4586	-2.2552	0.1278	2.3342	-2.1311
100	1	0	0.1894	0.0635	0.1269	0.1624	0.0671	0.2174	0.1475	0.0756
	10	0	0.4979	-0.2714	0.1188	0.4451	-0.2275	0.2046	0.3988	-0.1829
	100	0	1.1911	-0.9808	0.0989	1.1292	-0.9217	0.1734	1.0428	-0.8349
	1000	0	2.5048	-2.3011	0.0706	2.4397	-2.2367	0.1261	2.3044	-2.1009

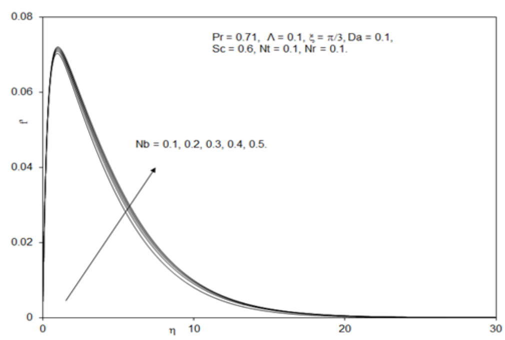

Fig. 3. Influence of Nb on velocity profile.

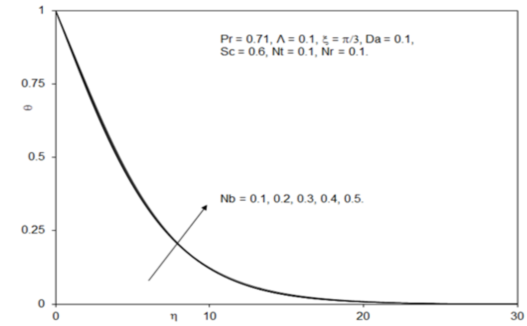

Fig. 4. Influence of Nb on temperature distribution.

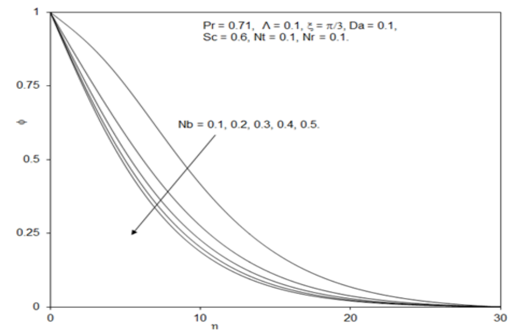

Fig. 5. Influence of Nb on nanofluid volume fraction.

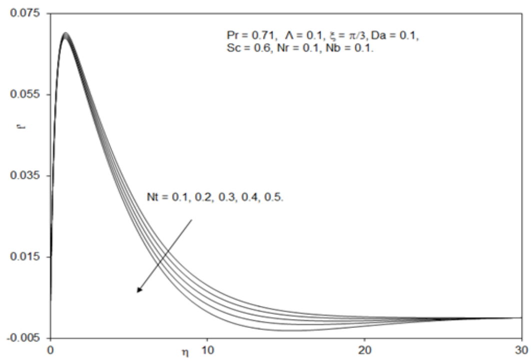

Fig. 6. Influence of Nt on velocity profile.

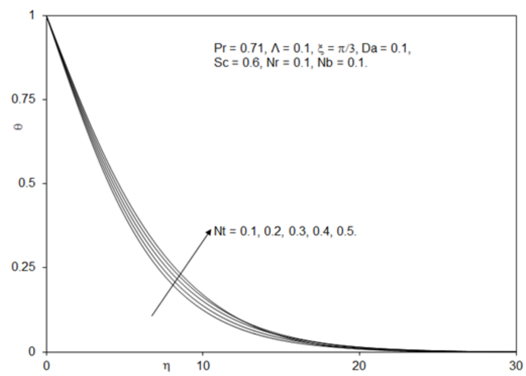

Fig. 7. Influence of Nt on temperature distribution.

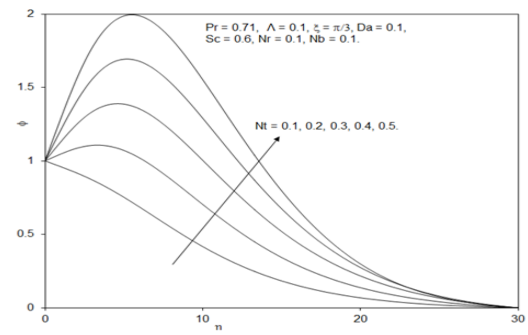

Fig. 8. Influence of Nt on nanofluid volume fraction.

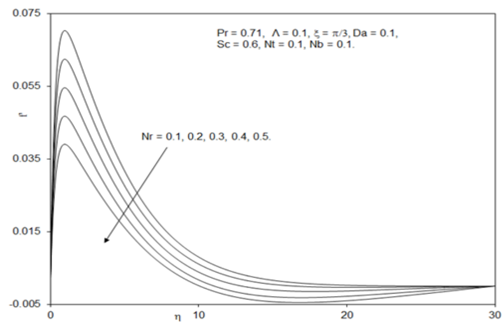

Fig. 9. Influence of Nr on velocity profile.

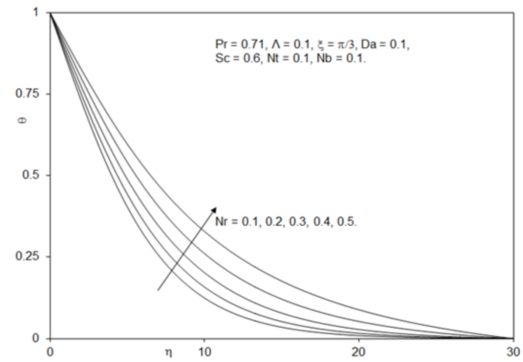

Fig. 10. Influence of Nr on temperature distribution.

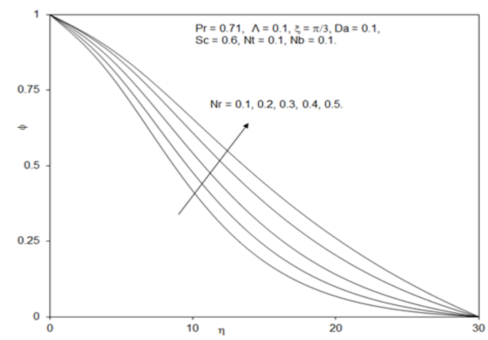

Fig. 11. Influence of Nr on nanofluid volume fraction.

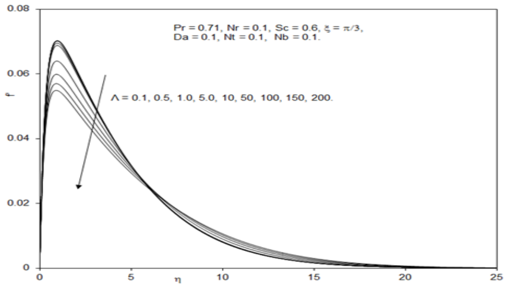

Fig. 12. Effect of Λ on velocity profile.

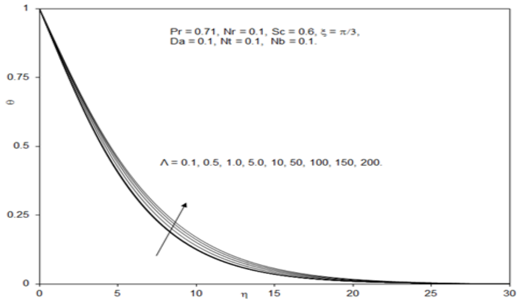

Fig. 13. Effect of Λ on temperature distribution.

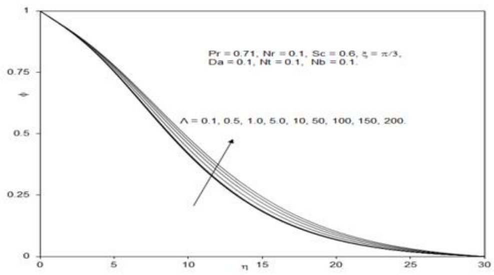

Fig. 14. Influence of Λ on nanofluid volume fraction.

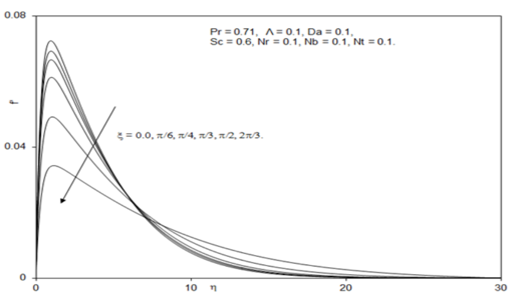

Fig. 15. Influence of ξ on velocity profile.

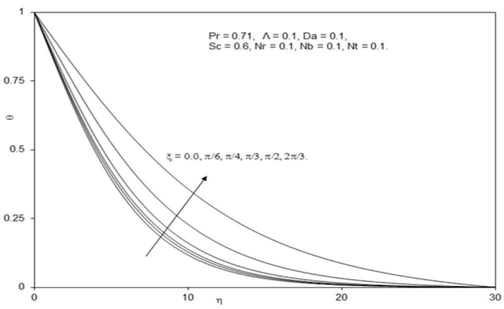

Fig. 16. Impact of ξ on temperature distribution.

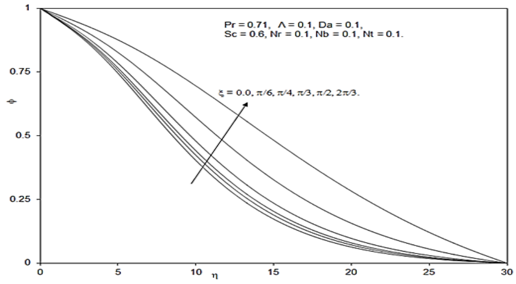

Fig. 17. Impact of ξ on nanofluid volume fraction.

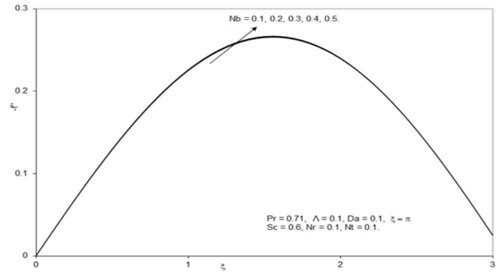

Fig. 18. Behaviour of local skin friction coefficient for various Nb.

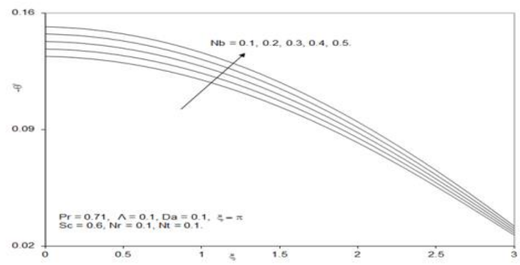

Fig. 19. Behavior of local Nusselt number for different Nb.

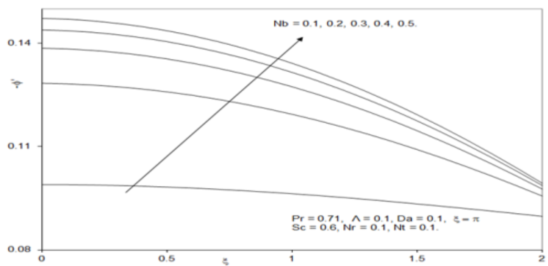

Fig. 20. Behaviour of $-\phi'(\xi,0)$ results for different Nb.

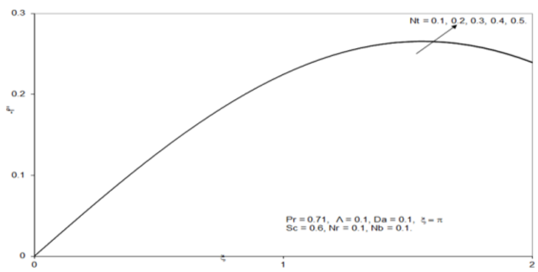

Fig. 21. Behaviour of local skin friction coefficient for different Nt.

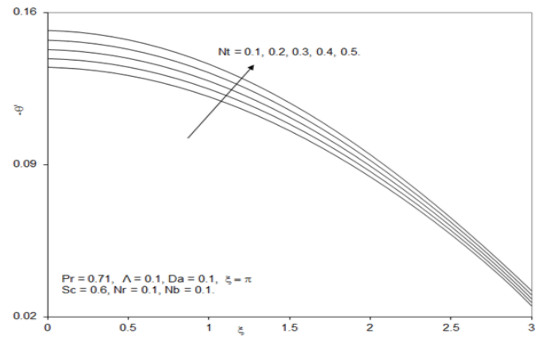

Fig. 22. Behavior of $-\theta'(\xi,0)$ results for different Nt.

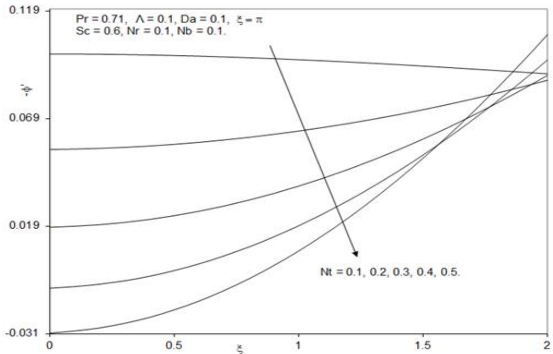

Fig. 23. Behavior of $-\phi'(\xi,0)$ results for different Nt.

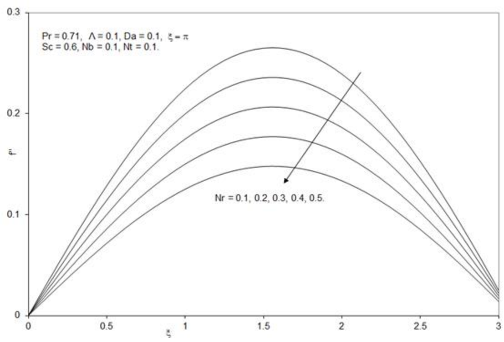

Fig. 24. Behavior of local skin friction coefficient for various Nr.

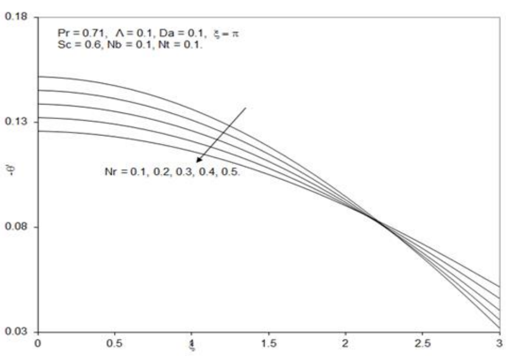

Fig. 25. Behavior of $-\theta'(\xi,0)$ results for different Nr.

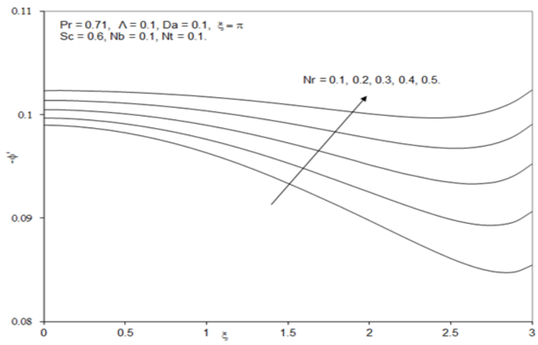

Fig. 26. Behavior of local Sherwood number results for different Nr.

6. Conclusions

In this study, the numerical investigation of free convection of nanofluid flow past a horizontal circular cylinder embedded in a non-Darcy porous medium is conducted. Buongiorno-Forchheimer model is employed for nanofluid flow modeling in a porous medium. The transformed nonlinear system is solved using Keller's-box method. Furthermore, validation of current solutions is done by comparing it with the existing solution in the literature. The important outcomes can be concise as:

1. Velocity and temperature are increases with increase in Nb but nanoparticle volume fraction decreases.
2. As thermophoresis increases the heat transfer increases in the boundary layer, and simultaneously intensifies particle deposition from the fluid region, leading to an increase in nanoparticle volume fraction.
3. With the increase in the buoyancy ratio parameter, the velocity profile strongly increases the boundary layer regime.
4. It is evident that increasing Λ clearly swamps the nanofluid momentum development, decreases the flow for some distance near the cylinder viscous region, later reverses the trend, and asymptotically reaches the far-field flow velocity.
5. The gradients of flow (i. e. $f''(\xi,0)$, $-\theta'(\xi,0)$ and $-\phi'(\xi,0)$) are enhanced along the surface of cylinder with increase in nanofluid slip parameters (Nt and Nb).

References

[1] S. U. S. Choi, "Enhancing thermal conductivity of fluids with nanoparticle", The *Proc. of the ASME Int. Mech. Eng. Congress and Exposition San Francisco*, pp. 99–105, (1995).

[2] F. C. Wang and H. A. Wu, "Enhanced oil droplet detachment from solid surfaces in charged nanoparticle suspensions", *Soft Matter*, Vol. 9, No. 33, pp.7974–7980, (2013).

[3] F. C. Wang and H. A. Wu, "Molecular dynamics studies on spreading of nanofluids promoted by nanoparticle adsorption on solid surface", *Theor. Appl. Mech. Lett.*, Vol. 3, No. 5, pp. 054006, (2013).

[4] Y. M. Xuan and W. Roetzel, "Conceptions for heat transfer correlation of nanofluids", *Int. J. Heat Mass Transfer*, Vol. 43, No. 19, pp. 3701–3707, (2006).

[5] J. Buongiorno "Convective transport in nanofluids" *J. Heat Transfer Trans. ASME*, Vol. 128, No. 3, pp. 240–250, (2006).

[6] O. Anwar Bég, V. R. Prasad, and B. Vasu., "Numerical study of mixed bioconvection in porous media saturated with nanofluid containing oxytactic microorganisms" *J. Mech. Med. Biol.*, Vol. 13 No. 4, pp. 1350067, (2013).

[7] S. Das, S. Chakraborty, R. N. Jana and O. D. Makinde, "Entropy analysis of unsteady magneto-nanofluid flow past accelerating stretching sheet with convective boundary condition", *Appl. Math. Mech.*, Vol. 36, No. 12, pp. 1593-1610, (2015).

[8] M. Sheikholeslami, D. D. Ganji, "Nanofluid convective heat transfer using semi analytical and numerical approaches: a review", *J. Taiwan Inst. Chem. Eng.*, Vol. 65, pp. 43-77, (2016).

[9] R. S. R. Gorla, B. J. Gireesha, and B. Singh, "MHD flow and heat transfer of dusty nanofluid embedded in porous medium over an exponentially stretching sheet", *J. Nanofluids (American Scientific Publishers)*, Vol. 4, No. 4, pp. 112, (2016).

[10] P. V. S. Murthy, A. Sutradhar, Ch. RamReddy, "Double-diffusive free convection flow past an inclined plate embedded in a non-Darcy porous medium saturated with a nanofluid" *Transfer porous. media*, Vol. 98, No. 3, pp. 553-564, (2013).

[11] P. Besthapu, R. U. Haq, S. Bandari, and Q. M. Al-Mdallal, "Mixed convection flow of thermally stratified MHD nanofluid over an exponentially stretching surface with viscous dissipation effect", *J. Taiwan Inst. Chem. Eng.*, Vol. 71, pp. 307-14, (2017).

[12] A. M. Aly, "Natural convection over circular cylinders in a porous enclosure filled with a nanofluid under thermo-diffusion effects," *J. Taiwan Inst. Chem. Eng.*, Vol. 70, pp. 88-103, (2017).

[13] M. A. Ahmadi, M. H. Ahmadi, M. F. Alavi, M. R. Nazemzadegan, R. Ghasempour, and S. Shamshirband, "Determination of thermal conductivity ratio of CuO/ethylene glycol nanofluid by connectionist approach," *J. Taiwan Inst. Chem. Eng.*, Vol. 91, pp. 383-395, (2018).

[14] D. A. Nield, and A. V. Kuznetsov, "The Cheng-Minkowycz problem for natural convection boundary-layer flow in a porous medium saturated by a nanofluid," *Int. J. Heat Mass Transfer*, Vol. 52, No. 25-26, pp. 5792-5795, (2009).

[15] P. Cheng and W. J. Minkowycz, "Free convection about a vertical flat plate embedded in a porous medium with application to heat transfer from a dike", *J. Geophys. Res.*, Vol. 82, No. 14, pp. 2040-2044, (1977).

[16] L. H. S. Roblee, R. M. Baird, and J. W. Tierney, "Radial porosity variations in packed beds," *AIChE J.*, Vol. 4, No. 4, pp. 460-464, (1958).

[17] K. Vafai, "Convective flow and heat transfer in variable-porosity media," *J. Fluid Mech.*, Vol. 147, pp. 233-259, (1984).

[18] J. Zueco, O. A. Bég, and H. S. Takhar, "Network numerical analysis of magneto-

micropolar convection through a vertical circular non-Darcian porous medium conduit", *Comput. Mater. Sci.*, Vol. 46, No. 4, pp. 1028-1037, (2009).

[19] W. J., Minkowycz, and C. Ping, "Free convection about a vertical cylinder embedded in a porous medium", *Int. J. Heat Mass Transfer*, Vol. 19, No. 7, pp. 805-813, (1976).

[20] H. T. Alkasasbeh, M. Z. Salleh, R. Nazar, and I. Pop, "Numerical solutions of radiation effect on magnetohydrodynamic free convection boundary layer flow about a solid sphere with Newtonian heating", *Appl. Math. Sci.*, Vol. 8, No. 140, pp. 6989-7000, (2014).

[21] M. Kumari and G. Rama Subba Reddy, "MHD Boundary Layer Flow of a Non-Newtonian Nanofluid Past a Wedge", *J. Nanofluids*, Vol. 4, No. 1, pp. 73-81, (2015).

[22] K. Peri, B. Kameswaran Vasu, P. V. S. N. Murthy and G. Rama Subba Reddy,, "Mixed Convection from a Wavy Surface Embedded in a Thermally Stratified Nanofluid saturated Porous Medium with non-Linear Boussinesq Approximation", *Int Comm Heat and Mass Transf*er, Vol. 77, pp. 78-86, (2016).

[23] O. A. Bég, V. R. Prasad, B. Vasu and G. Rama Subba Reddy, "Computational modeling of magnetohydrodynamic convection from a rotating cone in orthotropic Darcian porous media", *J. Braz. Soc. Mech. Sci. Eng.*, Vol. 39, No. 6, pp. 2035-2054, (2017).

[24] B. Vasu, Ch. RamReddy, P. V. S. N. Murthy and G. Rama Subba Reddy, "Entropy generation analysis in nonlinear convection flow of thermally stratified fluid in saturated porous medium with convective boundary condition", *J. Heat Transfer*, Vol. 139, No. 9, pp. 091701, (2017).

[25] O. A. Bég, Tasveer A. Bég, A. Y. Bakier and V. Prasad, "Chemically-reacting mixed convective heat and mass transfer along inclined and vertical plates with Soret and Dufour effects: Numerical solutions", *Int. J. Appl. Math. Mech.*, Vol. 5, No. 2, pp. 39-57, (2009).

[26] S. Munawar, A. Mehmood and A. Ali, "Time-dependent flow and heat transfer over a stretching cylinder", *Chin. J. Phys.*, Vol. 50, No. 5, pp. 828-848, (2012).

[27] K. A. Yih, "Effect of uniform blowing/suction on MHD-natural convection over a horizontal cylinder: UWT or UHF", *Acta mech.*, Vol. 144, No. 1-2, pp.17-27, (2000).

[28] V. R. Prasad, B. Vasu, O. A. Beg and D. R. Parshad, "Thermal radiation effects on magnetohydrodynamic heat and mass transfer from a horizontal cylinder in a variable porosity regime", *J. Porous Media*, Vol. 15, No. 3, pp. 261-281, (2012).

[29] B. Vasu, V. R. Prasad and O. A. Beg, "Thermo-diffusion and diffusion-thermo effects on MHD free convective heat and mass transfer from a sphere embedded in a non-Darcian porous medium", *J. Thermodyn.*, Vol. 2012, (2012).

[30] P. V. Satya Narayana and B. Venkateswarlu. "Heat and mass transfer on MHD nanofluid flow past a vertical porous plate in a rotating system," *Front. Heat Mass Transfer (FHMT)*, Vol. 7, No. 8, pp. 1-10 (2016).

[31] P. V. Satya Narayana, B. Venkateswarlu, and S. Venkataramana. "Thermal radiation and heat source effects on a MHD nanofluid past a vertical plate in a rotating system with porous medium." *Heat Transfer—Asian Res.*, Vol. 44, No. 1, pp. 1-19, (2015).

[32] D. Harish Babu, K. A. Ajmath, B. Venkateswarlu and P. V. Narayana. "Thermal Radiation and Heat Source Effects on MHD Non-Newtonian Nanofluid Flow over a Stretching Sheet." *J. Nanofluids*, Vol. 8, No. 5, pp. 1085-1092, (2018).

[33] H. B. Keller, *A new difference method for parabolic problems*, J. Bramble (Editor), Numerical Methods for Partial Differential Equations, (1970).

[34] T. Cebeci and P. Bradshaw, *Physical and Computational Aspects of Convective Heat Transfer*, Springer, New York, (1984).

[35] T. C. Chiam, "The flat plate magnetohydrodynamic boundary layer flow with a step change in the magnetic field", *J. Phys. Soc. Jpn.*, Vol. 62, No. 7, pp. 2516-2517, (1993).

[36] D. A. S. Rees and I. Pop, "Boundary layer flow and heat transfer on a continuous moving wavy surface", *Acta Mech.*, Vol. 112, No. 1, pp. 149-158, (1995).

[37] O. A. Bég, H. S. Takhar, G. Nath and M. Kumari, "Computational fluid dynamics modeling of buoyancy-induced viscoelastic flow in a porous medium", *Int J. Appl. Mech. Eng.*, Vol. 6, No. 1, pp. 187-210, (2001).

[38] V. R. Prasad, B. Vasu, O. A. Beg and R. D. Prashad, "Thermal Radiation Effects on Magnetohydrodynamic Free Convection Heat and Mass Transfer from a Sphere in a Variable Porosity Regime", *Commun. Nonlinear Sci. Numer. Simul.*, Vol. 17, No. 2, pp. 654-671, (2012).

[39] O. Anwar Bég, V. Ramachandra Prasad, B. Vasu, N. Bhaskar Reddy, Q. Li and R. Bhargava, "Free Convection Heat and ass Transfer from an Isothermal Sphere to a Micropolar Regime with Soret/Dufour Effects", *Int. J. Heat Mass Transfer*, Vol. 54, No. 1-3, pp. 9-18, (2011).

[40] G. Rama Subba Reddy and B. Vasu, "Unsteady Convective Heat Transfer to a stretching surface in a non-Newtonian nanofluid", *J. Nanofluids*, Vol. 5, No. 4, pp. 581-594, (2016).

[41] G. Rama Subba Reddy, B. Vasu and S. Siddiqa, "Transient Combined Convective Heat Transfer overstretching surface in a non-Newtonian nanofluid using Buongiorno's model", *J. Appl. Math. Phys*., Vol. 4, No. 2, pp. 443-460, (2016).

[42] J. H. Merkin, "Free convection boundary layers on cylinders of elliptic cross ction", *J. Heat Transfe*r, Vol. 99, pp. 453-457, (1977).

How to cite this paper:

B. Vasu and Atul Kumar Ray, " Novel numerical solution of non-linear heat transfer of nanofluid over a porous cylinder: Buongiorno-Forchheimer model,", *J. Comput. Appl. Res. Mech. Eng.*, Vol. 10, No. 2, pp. 473-496, (2021).

DOI: 10.22061/jcarme.2019.4320.1520

URL: https://jcarme.sru.ac.ir/?_action=showPDF&article=1059